Title: "Epigenome-wide methylation profile of chronic kidney disease-derived arterial DNA uncovers novel pathways in disease-associated cardiovascular pathology."

Athina Dritsoula[1], Maria Kislikova[1,2], Amin Oomatia[1], Amy Philomena Webster[3], Stephan Beck[3], Markella Ponticos[4], Ben Lindsey[1], Jill Norman[1], David C. Wheeler[1], Thomas Oates[1,5], Ben Caplin[1]

[1]Department of Renal Medicine, Division of Medicine, UCL, London, UK

[2]Department of Nephrology, University Hospital Marqués de Valdecilla, University of Cantabria, IDIVAL, Santander, Spain

[3]Department of Cancer Biology, Cancer Institute, UCL, London, UK

[4]Centre for Rheumatology and Connective Tissue Diseases, Division of Medicine, UCL, London, UK

[5]Departments of Nephrology and General Medicine, Royal London Hospital, Barts Health NHS Trust, London, E1 1BB

Corresponding author: Athina Dritsoula, athina.dritsoula.09@ucl.ac.uk, Department of Renal Medicine, Division of Medicine, UCL, London, UK, http://orcid.org/0000-0003-4225-6605

Short title: Arterial DNA methylation in CKD

Key words: Chronic kidney disease (CKD), cardiovascular disease (CVD), vascular remodeling, arterial aging, DNA methylation, epigenetics

Abstract word count: 247

Main text word count excluding references: 3900

Abstract

Chronic kidney disease (CKD) related cardiovascular disease (CVD) is characterized by vascular remodeling with well-established structural and functional changes in the vascular wall such as arterial stiffness, matrix deposition and calcification. These phenotypic changes resemble pathology seen in aging, and are likely to be mediated by sustained alterations in gene expression, which may be caused by epigenetic changes such as tissue-specific DNA methylation. We aimed to investigate tissue specific changes in DNA methylation that occur in CKD-related CVD. Genome-wide DNA methylation changes were examined in bisulfite converted genomic DNA isolated from the vascular media of CKD and healthy arteries. Methylation-specific PCR was used to validate the array data, and the association between DNA methylation and gene and protein expression was examined. The DNA methylation age was compared to the chronological age in both cases and controls. 319 differentially methylated regions (DMR) were identified spread across the genome. Pathway analysis revealed that DMRs associated with genes were involved in embryonic and vascular development, and signaling pathways such as TGFβ and FGF. Expression of top differentially methylated gene *HOXA5* showed a significant negative correlation with DNA methylation. Interestingly, DNA methylation age and chronological age were highly correlated, but there was no evidence of accelerated age-related DNA methylation in the arteries of CKD patients. In conclusion, we demonstrated that differential DNA methylation in the arterial tissue of CKD patients represents a potential mediator of arterial pathology and may be used to uncover novel pathways in the genesis of CKD-associated complications.

Introduction

Chronic kidney disease (CKD) is the syndrome characterized by reduced eGFR and kidney damage following a wide-range of different underlying diseases. Cardiovascular disease (CVD) is the primary cause of morbidity and mortality among patients with CKD (1). In CKD-related CVD, structural and morphological changes occur in the blood vessels leading to arterial stiffness, matrix deposition and calcification (2). These changes are underpinned by the activation of vascular smooth muscle cells (VSMC), which alter the extracellular matrix (ECM) component causing vascular remodeling (3). Recently, it has been suggested that these vascular changes represent accelerated aging (4, 5). Taken together, these phenotypic changes are likely to be a consequence of sustained alterations in gene expression. Inflammation, oxidative stress and other consequences of uremia that are evident in CKD induce epigenetic changes (6), including DNA methylation, histone modifications and non-coding RNAs, hence epigenetic modifications are mechanisms through which these long-term phenotypic changes might occur.

In mammals, DNA methylation classically occurs either at cytosine bases of CpG sites that are found spread out across the genome or in or near CpG islands, which are located close to transcription start sites or other regulatory regions. Although DNA methylation is traditionally associated with repression of gene expression in both cases, there is increasing evidence of both down- and up- regulation of gene expression (7). While aging is associated with an overall decrease in global DNA methylation, it can also increase or decrease at specific loci and such changes have been proposed to predispose to diseases of aging including cancer and metabolic disease (8).

A number of studies have demonstrated changes in DNA methylation in patients with CKD although these have been limited to interrogating leucocyte and/or kidney tissue DNA methylation (9-14). Furthermore, the largest of these studies with longitudinal follow-up suggests the majority of these changes were a consequence of impaired kidney function rather than a cause (11), implying that DNA methylation might be a key mechanism mediating the relationship between CKD and CKD-associated complications, including CKD-related CVD. Finally, it is clear that DNA methylation is not only time-dependent but also subject to substantial tissue-specific variation, meaning that understanding the contribution of epigenetic mechanisms to pathology requires the interrogation of the tissue of interest (15).

We hypothesized that the changes observed in the arterial wall in CKD-related CVD are mediated through DNA methylation of regulatory elements of key genes implicated in the pathobiology of disease and that understanding which genes and pathways are subject to this epigenetic regulation might provide key insight into CKD-related CVD. We aimed to describe genome-wide differences in arterial wall DNA methylation in patients with CKD versus healthy controls. We then validated the observed differentially methylated regions using methylation-specific PCR and assessed the downstream impact on gene and protein expression. Finally, we explored the relationship between DNA methylation patterns observed in CKD and those that occur in otherwise healthy aging.

Results

Participants

Thirty-two individuals contributed specimens for this study, of whom 25 were CKD patients and 7 were healthy donors. The study groups are summarized in Table 1.

Mean age was 48.2 years in cases and 51.14 years in controls. The percentage of male and female participants was similar between groups. Half of the CKD patients (48%) were on dialysis.

Table 1. *Demographic data*. Mean age is given in years. CKD= chronic kidney disease patients, Control= healthy donors, CI= 95% confidence interval.

Characteristic		CKD	Control
Number of specimens		25	7
Mean age (SD) (in years)		48.2 (±15)	51.14 (±11.6)
Sex (%)	Men	18 (72%)	5 (71%)
	Women	7 (28%)	2 (29%)
Smoking (%)		1 (4%)	0
Diabetes (%)		1 (4%)	0
Dialysis (%)		12 (48%)	0
Caucasian		16 (65%)	3 (42%)

Differentially methylated regions of arterial DNA potentially identify known and new disease-related pathways

We used the EPIC genome-wide methylation array to access the methylation status of DNA isolated from the VSMC of CKD patients and healthy subjects (Figure 1A). Four thousand and five hundred (4.5k) differentially methylated probes (DMP),

hypermethylated (Δβ<0) or hypomethylated (Δβ>0) in CKD, reached the genome-wide significance p-value (cut-off p-value< 9×10^{-8}) (16) (Figure 1B). The differentially methylated probes encompassed 319 differentially methylated regions (DMR). DMRs were found across the genome in all autosomal chromosomes (Figure 1C), with 87% of them being directly associated with genes (Figure 1D). Strong enrichment was seen near promoters, exons, introns and intron/exon junctions (Figure 1D). The remaining 13% were associated with CpG islands, island shores and shelves (up to 2Kb and 4Kb from the CpG island respectively (17)), and inter-island regions (Figure 1D).

Gene set enrichment and gene ontology analysis revealed that genes associated with DMRs participate in pathways related to embryonic development and morphogenesis (*NKX2-6*, *WNT5A*,*TWIST1*, etc), regulation of vascular development (*GATA3/4/5*, *FGFR2*, etc), cell proliferation and migration (*SMAD3*, *CAV1*, *PDGFRA*, etc), as well as signaling pathways such as TGFβ, FGF, Rho signaling and others (Figure 1E). Top hypermethylated and hypomethylated probes are shown in Table 2. Interestingly, among the top differentially methylated regions are found genes and homeobox containing transcription factors with established roles in embryonic development and maturation of the vascular system (Table 3).
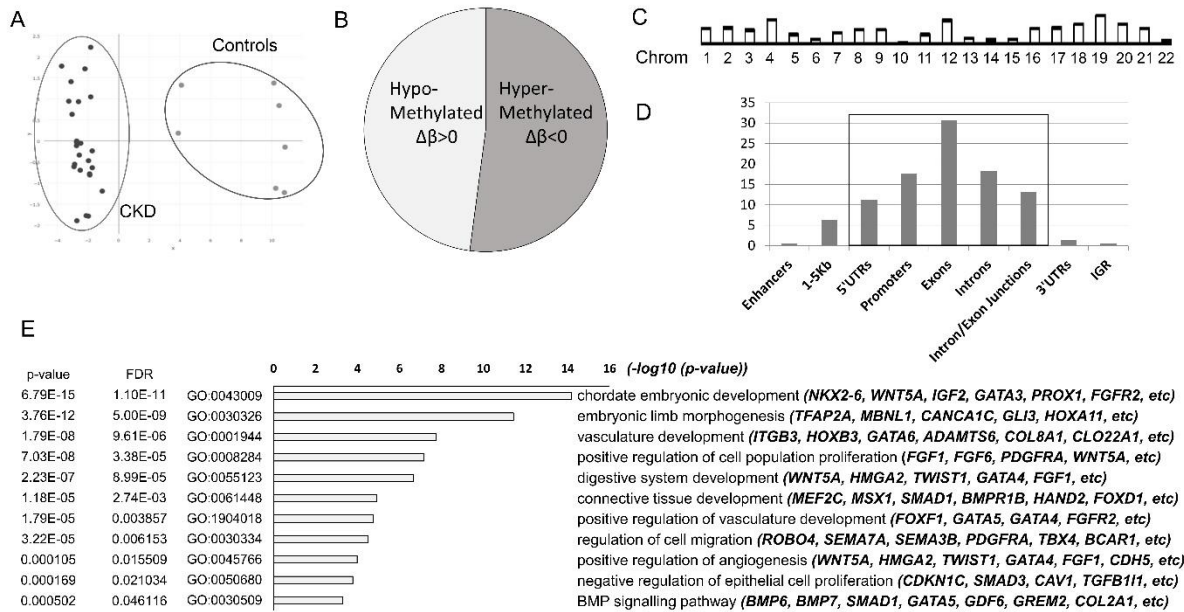
Figure 1. *Annotation of differentially methylated probes and regions.* A. Cluster plot for CKD and control samples based on their methylation profiles. B. Pie chart of 4.5k DMPs that reached genome-wide significance (p-value $<9 \times 10^{-8}$) showing percentage of hypermethylated (52%) and hypomethylated (48%) probes. C. Bar plot showing the position of the DMRs across the human genome in the autosomal chromosomes. D. Basic annotation of the DMRs in relation to genomic regions. Y axis: % enrichment normalized to background. E. Gene set enrichment and gene ontology analysis showing lead gene ontology categories (biological processes), and representative genes per category. X axis: $-\log_{10}$ of the adjusted p-values.

Table 2. *List of top differentially methylated probes (DMP).* Hypo- and hyper-methylated probes are shown based on their adjusted p-values. Δβ value shows the methylation difference of CKD and control samples. DMP-associated genomic regions and/or genes are shown. Chrom: chromosome, IGR: intergenic region, UTR: untranslated region. TSS1500: 1500bp from the transcription start site.

		Adjusted P-Value	Δβ	Chrom	Gene	Gene area	CpG Island relative area
Hypermethylated (Δβ<0)	cg05221631	7.78E-11	-0.18062	1	SMYD3	Body	opensea
	cg02766704	3.60E-09	-0.26897	7	CTTNBP2	Body	opensea
	cg22845765	4.22E-09	-0.17984	5		IGR	opensea
	cg07766803	4.22E-09	-0.12665	5	IRX2	3'UTR	shore
	cg02472525	8.27E-09	-0.12372	1	PALMD	Body	opensea
	cg10096519	1.03E-08	-0.15566	2	AGAP1	Body	shelf
	cg18835300	1.03E-08	-0.08739	4	PCDH7	Body	opensea
	cg05917748	1.10E-08	-0.19499	15		IGR	opensea
	cg12563935	1.20E-08	-0.05681	17	RGS9	Body	opensea
	cg07901514	1.25E-08	-0.15683	2		IGR	opensea
Hypomethylated (Δβ>0)	cg11761190	4.22E-09	0.176444	12		IGR	opensea
	cg05599870	1.10E-08	0.26365	8	CSMD3	Body	opensea
	cg03223959	1.20E-08	0.213298	16		IGR	opensea
	cg04902958	1.20E-08	0.194393	2		IGR	opensea
	cg05241044	1.27E-08	0.224311	4	GATB	Body	opensea
	cg26389913	1.35E-08	0.415965	12		IGR	opensea
	cg07206827	1.37E-08	0.22595	1	LINGO4	TSS1500	opensea
	cg15739591	1.37E-08	0.203465	7		IGR	opensea
	cg03372174	1.50E-08	0.15964	13		IGR	opensea
	cg03193356	1.92E-08	0.089679	8		IGR	opensea

Table 3. *Lead differentially methylated regions (DMR).* Lead DMRs based on their adjusted p-values (Bumphunter p-value area). The name of the genes associated with each DMR is given, as well as the chromosomal location, the genomic region, and the number of probes (DMPs) found in each DMR.

DMRs	Chrom	Adjacent Gene Name	Start position	End position	DMR width	Gene Area	No of probes in DMR	P-value Area
DMR_1	chr7	HOXA10-AS	27207996	27209828	1832	Intergenic	23	$<10^{-6}$
DMR_2	chr11	ALX4	44332332	44333192	860	Promoter	30	$<10^{-6}$
DMR_3	chr5	IRX2	2753746	2754322	576	Intron	10	7.53E-06
DMR_4	chr1	HLX	221053597	221055097	1500	Intron/Exon Junction	12	5.27E-05
DMR_5	chr4	MSX1	4863678	4864902	1224	Intron/Exon Junction	16	6.78E-05
DMR_6	chr12	Intergenic	115134148	115135333	1185	Intergenic	27	0.000112939
DMR_7	chr4	HAND2	174452461	174453287	826	Intron	9	0.000195761
DMR_8	chr5	C5orf66	134366162	134367680	1518	Intron/Exon Junction	9	0.000346346
DMR_9	chr5	PITX1	134363053	134363973	920	3' UTR	7	0.000798103
DMR_10	chr12	HOXC4	54446019	54446308	289	5' UTR	7	0.000843278
DMR_11	chr6	EYA4	133561368	133562101	733	Promoter/ 1st Exon	17	0.0006780
DMR_17	chr7	HOXA5	27183701	27185732	2031	Intergenic	33	0.000293642

Validation of the methylation array data using MSP

To validate the methylation array data, methylation-specific PCR (MSP) was used. Primers for randomly selected DMRs were specifically designed to amplify methylated and unmethylated DNA (Figure 2A). Methylation levels in MSP were consistent with the array data and showed a strong positive correlation in most cases studied (DMR 8: Spearman r=0.75, p-value=0.0007, DMR 9: Spearman r=0.71, p-value=0.0019) (Figure 2B-C, Supplementary Figure 1). DMRs 8 and 9 were both found hypermethylated in CKD cases compared to healthy individuals in the EPIC array (DMR 8: adjusted p-value=1.48E-05, DMR 9 adjusted p-value= 4.43E-05) (Supplementary Figure 1A). DMR 8 spans a 1.5kb long genomic region containing a CpG island that crosses intron/exon junctions of the overlapping *C5orf66* and *PITX1* genes, while DMR 9 is found at the 3' UTR of *PITX1* gene. These data confirm that the methylation array reproducibly captures the quantitative methylation status of loci across the human genome in the arterial tissue using our sample pipeline.
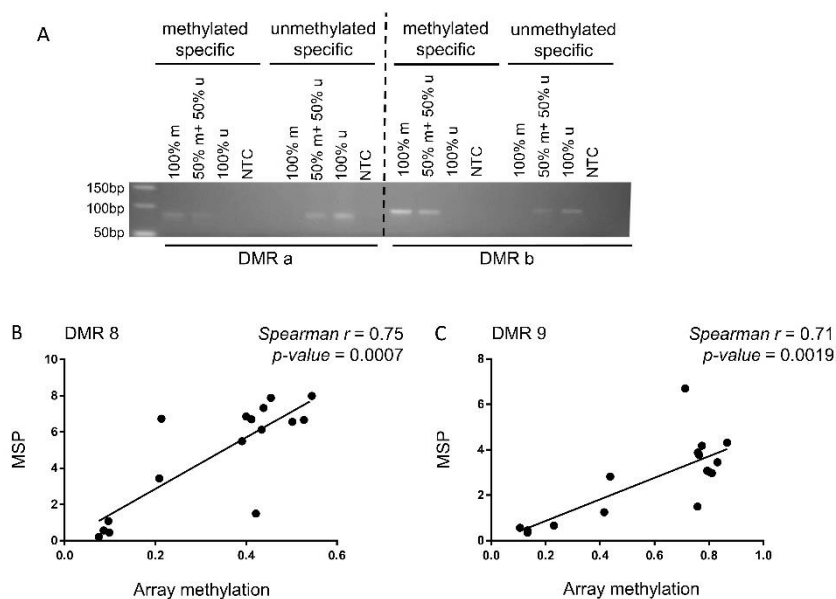
Figure 2. *Methylation specific PCR (MSP).* A. Primers were designed to specifically amplify methylated and unmethylated DNA. Control 0% (100% u) and 100% (100% m) methylated DNA samples were used individually or at a ratio of 50:50 to assess the dose-response across methylation levels. B-C: correlation analysis of methylation using MSP (y axis) and EPIC array methylation (x axis). r: Spearman correlation coefficient.

Association of DNA methylation and gene and protein expression

To further look into the biological relevance of DNA methylation, gene expression levels of differentially methylated genes were examined. Genes were selected from the top 60 DMRs based on the differential methylation levels, the location of each DMR, and the annotated gene function and properties. Gene expression was tested for the *HOXA5*, *HLX*, *HAND2*, *SLC41A3*, *SVIL* and *FMOD* genes, and correlated with the EPIC array methylation values of the corresponding DMRs (Figure 3 and Supplementary Figure 2).

HOXA5 gene and protein expression (qPCR and immunohistochemistry, respectively) was strongly negatively correlated with DMR 17 methylation values (p-value= 0.043, p-value= 0.03, respectively) (Figure 3), suggesting a direct effect of DNA methylation on gene expression. DMR 17 is located at the promoter of *HOXA5* gene and was found hypermethylated in CKD in the EPIC array. When *HOXA5* gene expression was examined, it was found significantly downregulated in CKD (Supplementary Figure 3). There was a suggestion for downregulation of HOXA5 protein in CKD, but the difference in expression did not reach statistical significance (Supplementary Figure 3).
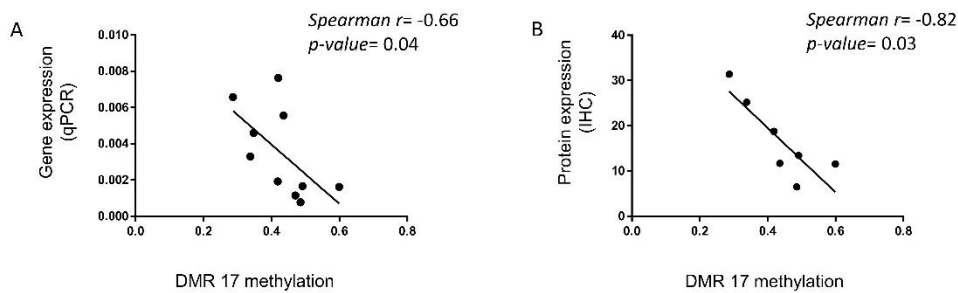
Figure 3. *DNA methylation associates with HOXA5 gene and protein expression.* Correlation of (A) *HOXA5* gene expression in VSMC, normalized to housekeeping genes and (B) HOXA5 protein expression, assessed by immunohistochemistry with the EPIC methylation array values of the corresponding DMR 17. r: Spearman correlation coefficient.

The changes in DNA methylation in the arterial wall of patients with CKD do not parallel those observed in aging

Using the methylation values of the EPIC array and the "Horvath clock", a tissue-independent age predictor (18), we calculated the estimated methylation age of the samples. The predicted methylation age was correlated well with the actual chronological age of the subjects in both cases and controls (Figure 4) (Spearman correlation r= 0.92, p-value <0.0001). However, no evidence of a higher DNA methylation age was found in CKD patients, suggesting that DNA methylation does not mediate a process of accelerating aging in the arteries of CKD patients.
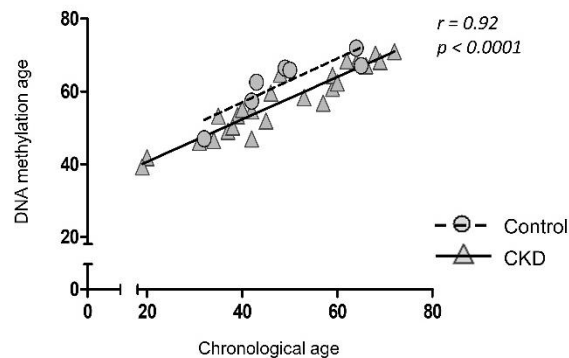
Figure 4. *DNA methylation age and chronological age are strongly correlated.* CKD: chronic kidney disease subjects, Control: healthy donors, r: Spearman correlation coefficient. Chronological age is presented in years.

Discussion

Although the exploration of epigenetic modifications in CKD has grown in the recent years, this is the first time that the methylation status of arterial wall DNA of CKD patients and healthy individuals has been quantified. Here, we examined the methylation status of VSMC at genome-wide level and we showed that there are approximately 319 large genomic regions and 4.5k probes that are differentially methylated in the arteries of patients with CKD. The regions are spread across the genome, and mostly found in or near genes, promoters and regulatory regions. The most significantly differentially methylated regions are associated with genes, processes and signaling pathways with roles in development, vasculature and fibrotic diseases.

In detail, differentially methylated genes are involved in the production and deposition of the extracellular matrix, encoding for collagenous and non-collagenous proteins

(*COL16A1, COL26A1, CLO6A3, COL7A1, COL9A3, COMP*), as well as proteins involved in the matrix deposition and degradation such as metalloproteinases and metallopeptidases (*ADAMTS8/9/12, MMP2, LOXL1*). Members of TGF-β, FGF, PDGF and Rho signaling pathways were also found to be differentially methylated in our dataset. In particular, signaling molecules of the TGFβ (*TGFβ1*, *TGFβ1l1*, *SMAD3*) and FGF (*FGF1*, *FGF6*, *FGFBP2*) pathways were all found hypomethylated in CKD. Interestingly, although CpG probes in or near *GATA5* were found significantly hypomethylated (eg. cg08583859, Δβ= 0.189, p-value= 3.81E-11), probes near *GATA4* were found both hypermethylated and hypomethylated in CKD, indicating a putative functional role for GATA binding site-dependent regulation. *RHOH* and *RHOJ* genes as well as other Rho/Ras family members (eg. *ARHGAP25, ARHGEF25)* were also found differentially methylated, contributing to the published evidence about the role of Rho signaling in the development and progression of vascular disease (19, 20). Interestingly, although recent evidence highlight the involvement of the immune system in the development of vascular disease (21), we confirmed that the effects seen in this study were driven by changes in the vascular media and not by infiltration of immune cells populations (Supplementary Figure 5) (22).

In contrast to a number of similar studies, we confirmed the accuracy of our array results at lead loci, demonstrating consistent changes in DNA-methylation using a MSP approach. Validation of the direction of array methylation using the MSP method might vary dependent of the locus of the methylated region in relation to the closest gene, with DMRs located in open sea/intragenic regions exhibiting indirect associations (Supplementary Figures 1A, 1B). We also showed that DNA methylation associates well with gene and protein expression at our lead locus, with HOXA5 gene and protein expression being downregulated (Supplementary Figure 3) in those

samples, following hypermethylation of the gene promoter. *HOXA5* encodes a homeobox transcription factor with important roles not only in embryonic development but also as a morphoregulatory gene in tissue remodeling, angiogenesis, and wound healing (23). A recent study speculated the role of *HOXA5* as an anti-atherogenic gene and showed that disturbed blood flow-dependent DNA methylation caused hypermethylation of *HOXA5* promoter and therefore silencing of gene expression (24). Hence, the data presented in this study in accordance with other published data support the role of *HOXA5* as a mechanosensitive gene and the concept that DNA methylation-dependent *HOXA5* repression contributes to pathologic tissue remodeling seen in CKD-related CVD leading to abnormal vasculature.

Similar analysis at other lead loci demonstrated unexpected results. DMR 7 is located 1-5Kb upstream of the *HAND2* gene transcription start site, and was found hypermethylated in CKD. However, hypermethylation at DMR 7 was associated with an increase in gene expression of the *HAND2* gene (Supplementary Figure 2). Interestingly, DMR 7 is also in close proximity to the *HAND2-antisense 1* gene, which shares a bidirectional promoter with *HAND2*. Although we could not demonstrate a clear association between methylation levels and expression of the anti-sense gene, these findings underline the complex-relationship between CpG methylation and expression of proximate genes and reinforce the importance of examining the impact of DNA-methylation on downstream biological pathways. In fact, the analysis of association between the location of the methylated DNA sites and gene expression has identified new patterns of methylation-mediated gene regulation including examples of methylation activating gene expression (25, 26). Studying expression of *HAND2* gene is a good example as there is accumulating evidence suggesting that gene expression is strongly regulated by DNA methylation in the context of other

diseases too (27). Other loci examined demonstrated quantitative trends toward inverse associations between gene-expression and methylation but not reaching thresholds for statistical significance (Supplementary Figure 2).

Furthermore, we aimed to address whether methylation changes in arterial DNA reflect epigenetic changes occurring in premature aging. We used the "Horvath" clock (18) to calculate the 'DNA-methylation age' for each sample, and as predicted, there was a strong correlation between methylation and chronological age across cases and controls. Interestingly, CKD-case status was not associated with an increase in 'DNA-methylation age' over healthy controls suggesting that CKD-associated arterial pathology is not a simplistic process of accelerated aging at least at the DNA methylation level. However, the "Horvath" clock is built as a pan-tissue clock programmed on differing tissue training sets, which reduces the possibilities of identifying aging-related changes associated with organ-specific pathologies (28). Therefore, using other disease-focused epigenetic clocks might capture the changes in accelerating aging that occur due to CKD-cardiovascular pathology (28).

The great majority of the published studies examining the epigenetic changes in CKD have been focused on the methylation status of DNA derived from whole blood, and to a lesser extent kidney tissue. In our study, we were interested in the association between methylation and CKD-related vascular complications, and therefore we aimed to assess the effect of DNA-methylation on gene and protein expression in VSMC. Our data are partially comparable with other published reports of differential DNA methylation in CKD in other tissues. In common with a previous report on DNA methylation of proximal tubule epithelial cells by Ko *et al* (10) our study confirmed that differentially methylated genes in CKD are associated with known players and regulators of cell adhesion, development-related functions and signaling pathways

involved in fibrosis, apoptosis and vasculature, such as collagen, fibronectin and other structural components, the TGFβ signalling pathway and SMAD proteins.

Another study by Smyth and colleagues was performed in leukocyte DNA to estimate the epigenetic features of CKD in which they identified twenty three differentially methylated genes with a strong biological and functional relevance to CKD pathogenesis (9). Evidence of differential DNA methylation of the *STK24* gene was replicated in our study, where the associated DMR 260 was also significantly hypermethylated in CKD. DMR 260 is located within an intron of the *STK24* gene, which encodes for a serine/threonine protein kinase mediating phosphorylation of MAP kinases. Furthermore, evidence of hypermethylation of cg19942083 in CKD, which was reported by Chu and colleagues (11), was also replicated in our study (Δβ= -0.0185). Association of increased methylation of this probe with prevalent CKD and estimated glomerular filtration rate (eGFR) has been replicated in two independent cohort studies and in a meta-analysis (corrected p-value= 2.8E-10) (11). Probe cg19942083 is located within an active enhancer between *PTPN6* and *PHB2* genes, and Chu *et al* showed that increased methylation at the locus is associated with increased eGFR as well as decreased expression of *PTPN6* gene and renal fibrosis (11). Interestingly, association of *PTPN6* differential methylation with eGFR was again recently replicated (29) supporting further the role of *PTPN6* gene as a promising candidate gene in kidney disease. Future studies are required to elucidate the role of these genes in the development and progression of cardiovascular pathology in CKD.

Key strengths of this study include the use of the EPIC array, which assesses the DNA methylation status at epigenome scale examining over 850k probes spread across the genome. Our key advantage compared to similar studies is the use of a specific tissue of interest that enabled us to directly associate successfully the effect of methylation

with gene and protein expression in the arterial wall. In addition, this approach facilitated our comprehension of the epigenetic phenomena and their relation to gene function and role in the CKD-related pathobiology.

The limited number of samples and the heterogeneous DNA material obtained from the healthy donors are some key downsides of this study. Nevertheless, the two groups of the study were clustered in two clear and very distinct populations based on their methylation profile. Another limitation is the lack of any hard clinical outcomes associated with CKD-related cardiovascular phenotypes among the CKD cases. Although this study provided evidence that DNA methylation status is a valuable tool to identify genes and mechanisms implicated in CKD-related CVD, further studies are required to determine whether the effect of DNA methylation retains a causal role or is an epiphenomenon of alternative underlying mechanisms and genome-epigenome crosstalk. Investigation of probes that exhibit clustered distribution in DNA methylation, known as "gap probes", will also aid this cause (30). DNA methylation signals of gap probes, which are usually associated with adjacent SNPs, have a strong genetic basis, and they can be used as reliable surrogates for underlying genetic structure that is biologically relevant to the phenotype. In our study, we have identified (30) a number of gap probes associated with differentially methylated loci, including probes in DMR 17, highlighting that potential genetic effects are present and need to be further investigated. Animal models of CKD-related CVD and mechanisms that block methylation, as well as further genetic annotation and analysis of the methylated loci could enlighten the role of DNA methylation in the cardiovascular component of CKD.

In summary, we have demonstrated differential DNA methylation at a range of loci in arterial tissue from patients with CKD as compared to healthy controls. These epigenetic changes represent a potential mediator of arterial pathology in those with

renal failure, which in turn may be a result of the uremic milieu or other consequences of advanced CKD. Our findings also suggest that CKD-associated CVD does not reflect epigenetic changes seen in aging and alternative paradigms should be sort. We established the use of profiling the epigenome-wide methylation status in CKD-derived arterial DNA as a proof of concept to uncover novel pathways in the genesis of CKD-associated complications.

Participants, Methods and Materials

Study participants and donation of arterial material

The study protocol was approved by the London - Queen Square Research Ethics Committee (ref: 16/LO/0269) and all participants provided written informed consent.

All cases were patients with end-stage renal disease undergoing live or cadaveric-donor single organ renal transplantation at the Royal Free London NHS Foundation Trust. At the time of surgery, a small portion (1-2cm) of inferior epigastric artery (IEA) was retrieved. Control samples were obtained from patients undergoing live kidney donation operations as well as tissue from the main renal artery of donated live and cadaveric donor kidneys (the latter not transplanted and donated for research). At surgery (at the discretion of the operating surgeon dependent on whether substantial additional dissection was required) either the IEA was divided, and portion retrieved (~1cm) or alternatively, excess material from the renal artery of the explanted kidney was collected for research. All specimens were placed in ice-cold saline before further processing. Basic demographic and clinical data were collected on all participants.

Tissue specimens

Within 1 hour of retrieval endothelial and adventitial layers were dissected off the arterial specimen. The remaining arterial media was either stabilized, in RNA later (Thermo Fisher, Cat. no: AM7020) or All Protect tissue reagent (Qiagen, Cat. no: 76405) for future isolation of nuclei acids, or fixed in formalin before transfer to ethanol for histological processing.

Nucleic acid isolation from human vessels

For the isolation of DNA and RNA the AllPrep DNA/RNA Mini kit (Qiagen, Cat. no: 80204) was used. DNA and RNA were isolated from the arterial media (vascular smooth muscle layer) of 25 recipients (CKD patients; IEA) and 7 donors (controls; IEA or renal artery) during kidney transplantation procedures. 0.3-0.6 mg of prepared vascular tissue was homogenised in 600 µl lysis buffer with stainless steel beads (Qiagen, Cat. no: 69989) using a conventional tissue-lyser. The samples were kept ice-cold during homogenisation. DNA and RNA were then isolated following the manufacturer's instructions. DNA was purified and concentrated by ethanol precipitation.

Bisulfite conversion of DNA

250ng DNA/sample was bisulfite-converted (EZ DNA Methylation kit, Zymo, Cat. no: D5001) and methylation status was assessed by the Illumina EPIC array (UCL Genomics Institute). For the methylation-specific PCRs DNA was bisulfite-converted following the same protocol.

Illumina methylation array analysis

The Illumina EPIC methylation array assessed over 850.000 methylation sites across the genome at single-nucleotide resolution. Methylation sites outside CpG islands, as

well as probes that span enhancers and promoters identified by ENCODE and FANTOM, open chromatin regions and DNase hypersensitivity sites are also included (31).

For the methylation data analysis and the identification of differentially methylated probes and regions, the ChAMP package was used exclusively in R 4.0 (32, 33). Failed probes (detection p-value <0.01), SNP-related probes (34), multi-hit probes (35), and probes located on the XY chromosomes were filtered out from the dataset. The methylation is measured using the beta (β) value, which ranges from 0 (no methylation) to 1 (100% methylation), and offers an intuitive biological interpretation. The type 2 probe bias was normalized using the BMIQ method (36). For the principal component analysis and the detection of batch effects, singular value decomposition (SVD) method was used (37), and the technical variation was corrected using ComBat (38) on the normalized values (Supplementary Figure 4). ComBat was performed once to correct the "array" batch variation only, as this was the batch with the biggest effect on the dataset. To prevent correction of batch effects that would be influenced by group differences in case of unbalanced group design, sample group was not included in the model matrix during ComBat analysis.

For the identification of the differentially methylated probes between CKD patients and healthy controls, the Limma package (39) was used implemented through ChAMP. Differentially methylated regions were identified using the Bumphunter algorithm (40), with each region containing a minimum of seven DMPs. The p-values were corrected using the "bootstrap" method through ChAMP. Gene enrichment analysis was performed using the "gometh" method of "missMethyl" package (41) through ChAMP. This method reduces significantly the bias during gene set analysis by adjusting the

number of CpGs attributed to a gene or locus. The list of DMRs was used as input for the Annotatr package (42) to dissect genomic annotations.

Methylation-specific PCR (MSP)

Methylation-specific PCRs were performed using the Epitect MSP kit (Qiagen, Cat. no: 59305). Two different sets of primers (Supplementary Table 1) were designed for each region, specific either to methylated or unmethylated DNA using the MethPrimer program (www.urogene.org). Most of the primers spanned at least one CpG to increase the primer specificity and efficiency to distinguish between methylated and unmethylated DNA. 2µl of bisulfite-converted DNA (~10ng) was used per MSP reaction. 100% methylated DNA and unmethylated DNA (0% methylation) were used as positive and negative control, respectively (Qiagen, Cat. no: 59568). MSP products were run in a 2% agarose gel, visualised and photographed using a UVP gel documentation system (BioSpectrum). Densitometry analysis was performed in ImageJ to infer the relative methylation of the locus per sample in relation to the positive (methylation value= 1) and negative control (methylation value= 0).

Immune cell population involvement

A cell-type fraction analysis was performed with EpiDISH (22) using the beta values of our dataset.

Gene expression analysis- Quantitative PCR

500ng RNA/sample was reverse transcribed following a standard protocol (Thermo Fisher, Cat. no: 4368814) in a total reaction volume of 100µl. 2µl of cDNA (1:10 dilution) was used per qPCR reaction (QuantiFast SYBR Green, Qiagen, Cat. no: 204054). Relative gene expression was normalised against the mean Ct of three

housekeeping genes: *RPL13*, *HPRT*, and *ACTB*. Primer sequences and annealing temperature for each primer pair are given in the Supplementary Table 2.

Immunohistochemistry

Immunohistochemistry was performed on formalin fixed paraffin-embedded epigastric arteries isolated during the kidney transplantation procedures. After antigen retrieval with 1mM EDTA pH 8.0, sections were immunodecorated with optimally diluted antibodies (HOXA5: sc-515309, Santa-Cruz, 0.5µg/ml in TBS). Labelled Polymer - Dako REAL EnVision-HRP (Dako, K4000) was used prior to developing with 3,3'-Diaminobenzidine (DAB) reagent (Dako, K3467). Specificity of staining was confirmed using isotype-matched IgG control antibodies (0.5µg/ml).

Statistical analysis

Tests for differences in CpG methylation at specific loci (as determined by MSP), gene and protein expression, between groups were performed using Student's t-test. The association between CpG methylation (assessed by EPIC array) and age, CpG methylation (by MSP), gene or protein expression was tested using Pearson correlation coefficient. The analysis was performed in GraphPad Prism 5. Post-hoc power calculations were performed using pwrEWAS (43).

Author contributions

BC conceived the study with assistance from JN, SB, DCW and MP. BL led the surgical aspects of the work. AD, MK and AO collected the samples and performed the laboratory procedures. AD performed the analysis with support from APW, TO and SB. AD and BC drafted the manuscript with support from SB and TO. All authors read and approved the final submission.

Disclosure Statement

No potential conflict of interest was reported by the authors.

1.   Go AS, Chertow GM, Fan D, McCulloch CE, Hsu CY. Chronic kidney disease and the risks of death, cardiovascular events, and hospitalization. N Engl J Med. 2004;351(13):1296-305.

2.   Blacher J, Guerin AP, Pannier B, Marchais SJ, London GM. Arterial calcifications, arterial stiffness, and cardiovascular risk in end-stage renal disease. Hypertension. 2001;38(4):938-42.

3.   Briet M, Burns KD. Chronic kidney disease and vascular remodelling: molecular mechanisms and clinical implications. Clin Sci (Lond). 2012;123(7):399-416.

4.   London GM, Safar ME, Pannier B. Aortic Aging in ESRD: Structural, Hemodynamic, and Mortality Implications. J Am Soc Nephrol. 2016;27(6):1837-46.

5.   Hamczyk MR, Nevado RM, Barettino A, Fuster V, Andrés V. Biological Versus Chronological Aging: JACC Focus Seminar. Journal of the American College of Cardiology. 2020;75(8):919-30.

6.   Zawada AM, Rogacev KS, Heine GH. Clinical relevance of epigenetic dysregulation in chronic kidney disease-associated cardiovascular disease. Nephrology Dialysis Transplantation. 2013;28(7):1663-71.

7.   Schübeler D. Function and information content of DNA methylation. Nature. 2015;517(7534):321-6.

8.   Bell CG, Beck S. The epigenomic interface between genome and environment in common complex diseases. Brief Funct Genomics. 2010;9(5-6):477-85.

9.   Smyth LJ, McKay GJ, Maxwell AP, McKnight AJ. DNA hypermethylation and DNA hypomethylation is present at different loci in chronic kidney disease. Epigenetics. 2014;9(3):366-76.

10.   Ko YA, Mohtat D, Suzuki M, Park AS, Izquierdo MC, Han SY, et al. Cytosine methylation changes in enhancer regions of core pro-fibrotic genes characterize kidney fibrosis development. Genome biology. 2013;14(10):R108.

11.   Chu AY, Tin A, Schlosser P, Ko YA, Qiu C, Yao C, et al. Epigenome-wide association studies identify DNA methylation associated with kidney function. Nat Commun. 2017;8(1):1286.

12.   Wing MR, Devaney JM, Joffe MM, Xie D, Feldman HI, Dominic EA, et al. DNA methylation profile associated with rapid decline in kidney function: findings from the CRIC study. Nephrol Dial Transplant. 2014;29(4):864-72.

13.   Sapienza C, Lee J, Powell J, Erinle O, Yafai F, Reichert J, et al. DNA methylation profiling identifies epigenetic differences between diabetes patients with ESRD and diabetes patients without nephropathy. Epigenetics. 2011;6(1):20-8.

14.   Lecamwasam A, Sexton-Oates A, Carmody J, Ekinci EI, Dwyer KM, Saffery R. DNA methylation profiling of genomic DNA isolated from urine in diabetic chronic kidney disease: A pilot study. PLoS One. 2018;13(2):e0190280.

15.   Schultz MD, He Y, Whitaker JW, Hariharan M, Mukamel EA, Leung D, et al. Human body epigenome maps reveal noncanonical DNA methylation variation. Nature. 2015;523(7559):212-6.

16.   Mansell G, Gorrie-Stone TJ, Bao Y, Kumari M, Schalkwyk LS, Mill J, et al. Guidance for DNA methylation studies: statistical insights from the Illumina EPIC array. BMC genomics. 2019;20(1):366.

17.   Irizarry RA, Ladd-Acosta C, Wen B, Wu Z, Montano C, Onyango P, et al. The human colon cancer methylome shows similar hypo- and hypermethylation at conserved tissue-specific CpG island shores. Nature genetics. 2009;41(2):178-86.

18.   Horvath S. DNA methylation age of human tissues and cell types. Genome biology. 2013;14(10):R115.

19.   Zhou Q, Liao JK. Rho Kinase: An Important Mediator of Atherosclerosis and Vascular Disease. Curr Pharm Des. 2009;15(27):3108-15.

20.   Duluc L, Wojciak-Stothard B. Rho GTPases in the regulation of pulmonary vascular barrier function. Cell Tissue Res. 2014;355(3):675-85.

21.   Fani L, van der Willik KD, Bos D, Leening MJG, Koudstaal PJ, Rizopoulos D, et al. The association of innate and adaptive immunity, subclinical atherosclerosis, and cardiovascular disease in the Rotterdam Study: A prospective cohort study. PLoS medicine. 2020;17(5):e1003115.

22.   Zheng SC, Webster AP, Dong D, Feber A, Graham DG, Sullivan R, et al. A novel cell-type deconvolution algorithm reveals substantial contamination by immune cells in saliva, buccal and cervix. Epigenomics. 2018;10(7):925-40.

23.   Kachgal S, Mace KA, Boudreau NJ. The dual roles of homeobox genes in vascularization and wound healing. Cell Adh Migr. 2012;6(6):457-70.

24.   Dunn J, Qiu H, Kim S, Jjingo D, Hoffman R, Kim CW, et al. Flow-dependent epigenetic DNA methylation regulates endothelial gene expression and atherosclerosis. J Clin Invest. 2014;124(7):3187-99.

25.   Kulis M, Heath S, Bibikova M, Queiros AC, Navarro A, Clot G, et al. Epigenomic analysis detects widespread gene-body DNA hypomethylation in chronic lymphocytic leukemia. Nature genetics. 2012;44(11):1236-42.

26.   Spainhour JC, Lim HS, Yi SV, Qiu P. Correlation Patterns Between DNA Methylation and Gene Expression in The Cancer Genome Atlas. Cancer informatics. 2019;18:1176935119828776.

27.   Jones A, Teschendorff AE, Li Q, Hayward JD, Kannan A, Mould T, et al. Role of DNA methylation and epigenetic silencing of HAND2 in endometrial cancer development. PLoS medicine. 2013;10(11):e1001551.

28.   Bell CG, Lowe R, Adams PD, Baccarelli AA, Beck S, Bell JT, et al. DNA methylation aging clocks: challenges and recommendations. Genome biology. 2019;20(1):249.

29.   Chen J, Huang Y, Hui Q, Mathur R, Gwinn M, So-Armah K, et al. Epigenetic Associations with Estimated Glomerular Filtration Rate (eGFR) among Men with HIV Infection. Clin Infect Dis. 2019.

30.   Andrews SV, Ladd-Acosta C, Feinberg AP, Hansen KD, Fallin MD. "Gap hunting" to characterize clustered probe signals in Illumina methylation array data. Epigenetics & Chromatin. 2016;9(1):56.

31.   Pidsley R, Zotenko E, Peters TJ, Lawrence MG, Risbridger GP, Molloy P, et al. Critical evaluation of the Illumina MethylationEPIC BeadChip microarray for whole-genome DNA methylation profiling. Genome biology. 2016;17(1):208.

32.   Morris TJ, Butcher LM, Feber A, Teschendorff AE, Chakravarthy AR, Wojdacz TK, et al. ChAMP: 450k Chip Analysis Methylation Pipeline. Bioinformatics (Oxford, England). 2014;30(3):428-30.

33.   Aryee MJ, Jaffe AE, Corrada-Bravo H, Ladd-Acosta C, Feinberg AP, Hansen KD, et al. Minfi: a flexible and comprehensive Bioconductor package for the analysis of Infinium DNA methylation microarrays. Bioinformatics (Oxford, England). 2014;30(10):1363-9.

34.   Zhou W, Laird PW, Shen H. Comprehensive characterization, annotation and innovative use of Infinium DNA methylation BeadChip probes. Nucleic Acids Res. 2017;45(4):e22.

35.   Nordlund J, Backlin CL, Wahlberg P, Busche S, Berglund EC, Eloranta ML, et al. Genome-wide signatures of differential DNA methylation in pediatric acute lymphoblastic leukemia. Genome biology. 2013;14(9):r105.

36.   Teschendorff AE, Marabita F, Lechner M, Bartlett T, Tegner J, Gomez-Cabrero D, et al. A beta-mixture quantile normalization method for correcting probe design bias in Illumina Infinium 450 k DNA methylation data. Bioinformatics (Oxford, England). 2013;29(2):189-96.

37.   Teschendorff AE, Menon U, Gentry-Maharaj A, Ramus SJ, Gayther SA, Apostolidou S, et al. An epigenetic signature in peripheral blood predicts active ovarian cancer. PLoS One. 2009;4(12):e8274.

38.   Johnson WE, Li C, Rabinovic A. Adjusting batch effects in microarray expression data using empirical Bayes methods. Biostatistics. 2007;8(1):118-27.

39.   Ritchie ME, Phipson B, Wu D, Hu Y, Law CW, Shi W, et al. limma powers differential expression analyses for RNA-sequencing and microarray studies. Nucleic Acids Res. 2015;43(7):e47.

40.   Jaffe AE, Murakami P, Lee H, Leek JT, Fallin MD, Feinberg AP, et al. Bump hunting to identify differentially methylated regions in epigenetic epidemiology studies. Int J Epidemiol. 2012;41(1):200-9.

41.   Phipson B, Maksimovic J, Oshlack A. missMethyl: an R package for analyzing data from Illumina's HumanMethylation450 platform. Bioinformatics (Oxford, England). 2016;32(2):286-8.

42.   Cavalcante RG, Sartor MA. annotatr: Genomic regions in context. Bioinformatics (Oxford, England). 2017.

43.   Graw S, Henn R, Thompson JA, Koestler DC. pwrEWAS: a user-friendly tool for comprehensive power estimation for epigenome wide association studies (EWAS). BMC bioinformatics. 2019;20(1):218.